

Optical Properties of Lead-Phosphate Glasses Containing Barium, Magnesium, and Calcium Oxides

Dhyghm A. Ibrahim¹, Najat A. Dahham², Manaf A. Hassan³

¹ Tikrit University College of Science, Phys. Dept

² Tikrit University College of Science, Phys. Dept

³ University of Kirkuk, College of Education for Pure Science, Phys. Dept

Abstract

Glasses with compositions

X% BaO – 25% PbO – (75-X)% P₂O₅

X% CaO – 25% PbO – (75-X)% P₂O₅

X% MgO – 25% PbO – (75-X)% P₂O₅

Where $x = 5, 10, 15,$ and 20 mol%) were prepared by the convocal melt quenching method. The density, molar volume x -ray diffraction (XRD), optical energy band gap on IR Spectra of these glasses have been measured. The refractive index and molar refraction of oxide ion have been calculated by using Lorentz - Lorentz relations. Optical absorption Spectra of these glasses were recorded in the range (190-900)nm at room temperature. Refractive index (n) and optical energy bandgap (E_{opt}) agree well compared with other glasses. In directed allowed optical transitions are favorable in these glasses, and the optical band energy has been observed to decrease with an increase in BaO, MgO, and CaO content. Infrared IR spectroscopy showed that the addition of BaO, MgO, CaO does not introduce any new absorption band in lead phosphate oxide glasses.

Keyword: Optical properties, Oxide Glasses, Absorption Edge, lead phosphate oxide glasses,

I. Introduction

In amorphous as in crystalline materials, useful information can be deduced from the optical absorption edge and infrared absorption spectral measurements. Even though the edge is less sharp in such materials, the absorption peaks are broader than is normally the case for non-metallic crystals[1].

Optical absorption is a useful method for investigating optically induced transitions and getting information about the band structure and energy gap of non-crystalline materials [2]. This technique's principle is that a photon with energy greater than the bandgap energy will be absorbed.

Optical properties of various inorganic glasses containing different transition metal ions have been severely investigated [3-5]. Phosphate glasses are scientifically and technologically important because they generally offer some unique physical properties better than other glasses,

such as low melting and softening temperatures, high electrical conductivity, ultraviolet(UV) transmission, and optical characteristics [6-8].

Phosphate glass types are attractive hosts and are considered promising for optical amplifiers, fibers, and laser [9]. Many studies on the characterization of phosphate glass types proved that, by adding cation with a high value of electrostatic field strength like (Pb²⁺), the covalence of (P-O-M) bond increases [10,11].

Refractive index (n) is one of the important properties for optical glasses, and a large number of researchers [12,13] investigated the relation of refractive index with glass composition. It is generally recognized that the refractive index of many common glasses can be varied by changing the base glass compositions [29]. In this research, we have studied the change in the optical band gap, infrared spectroscopy investigation, refractive index, density, and molar volume due to increased BaO, MgO, and CaO in the glass_network.

II. Experimental

Glasses with compositions

X% BaO – 25% PbO – (75-X)% P₂O₅

X% CaO – 25% PbO – (75-X)% P₂O₅

X% MgO – 25% PbO – (75-X)% P₂O₅

Where $x=5, 10, 15,$ and 20 mol%, were prepared by using a conventional melt quenching method. Chemical powders of reagent grade P₂O₅, PbO, BaO, MgO, and CaO were mixed for three series of glasses and melted in alumina crucibles placed in an electrically heated muffle furnace at (900_1000)C° for (1h) preheated in an electric furnace for (1h) keeps at 250C° to minimize the volatilization. The melts were poured on to the stainless plate and pressed to a thickness of (2_3)mm at room temperature. The glass powder was mixed with spectroscopically pure KBr. The mixed glass samples were pressed in a die to obtain pellets and subjected to a pressure of 5tons/cm². The infrared (IR) transmission spectra of these glass pellets were measured at room temperature using Perkin Elmer FTIR spectrophotometer in the range (400_4000)cm⁻¹. X-ray diffraction measurements confirmed the glassy nature of all the samples examined. The samples' optical density was



measured as a function of wavelength using a Perkin_Elmer 402 spectrophotometer in the spectral range from 190 to 900 nm.

The density (ρ_G) of glass samples was determined using Archimede's principle with toluene as an inert buoyant liquid. The glass density (ρ_G) was determined by using the equation.

$$\rho_G = \frac{W_a}{W_a - W_L} (\rho_L) \dots\dots\dots(1)$$

Where (ρ_L) is the density of immersion liquid, which is toluene ($\rho_L=0.86\text{g/cm}^3$). (W_a) is the glass's weight in the air, and (W_L) is the sample's weight when immersed in the immersion liquid? The molar volume (V_m) is calculated by using the obtained density and weight of one mole of the sample by using the equation :

$$V_m = \sum_i \frac{X_i M_i}{\rho_G} \dots\dots\dots(2)$$

Where (X_i) and (M_i) refer to the molar fraction and molecular weight of the (i^{th}) of the component, respectively. The main feature of the absorption edge of amorphous semiconductors, particularly at the lower values of absorption of coefficient, is an exponential increase of the absorption coefficient $\alpha(\omega)$ with photon energy ($\hbar\omega$) in accordance with an empirical relation due to Urbach [16].

$$\alpha(\omega) = \alpha_o \exp(\hbar\omega/E_o) \dots\dots\dots(3)$$

Where(α_o) is a constant, (E_o) is the Urbach energy indicates the width of the localized states' band tails, and (ω) is the angular frequency of the radiation.

The absorption coefficient $\alpha(\omega)$ can be determined near the edge of the formula [17].

$$\alpha(\omega) = \frac{1}{d} \ln \frac{I_o}{I_t} \dots\dots\dots(4)$$

Where (d) is the thickness of the sample (I_o) and (I_t) are the intensities of the incident and transmitted beams, respectively. Davis and Mott [18] defined a plot of absorption coefficient $\alpha(\omega)$ versus photon energy to calculate the energy bandgap using the relation:

$$\alpha(\omega) = \frac{A}{\hbar\omega} (\hbar\omega - E_{opt})^r \dots\dots\dots(5)$$

Where (A) is a constant and (r) an index which can assume values of 1,2,3,1/2 and 3/2 depending on the nature of the interband electronic transitions. Such transitions are due to electromagnetic wave interaction with an electron that causes the electron in the valence band to jump the conduction band. The refractive index (n) is important to determine the local field effects of the material. The refractive index can be calculated by the equation [19]:

$$\frac{n^2-1}{n^2+2} = 1 - \sqrt{(E_{opt}/20)} \dots\dots\dots(6)$$

The Lorentz- Lorentz equation is used to calculate the molar refractivity (R_m) as follows [19]:

$$R_m = \frac{(n^2-1)}{(n^2+2)} V_m \dots\dots\dots(7)$$

III. Results and Discussion

A. Density Measurements

The calculated values of density (ρ_G) and molar volume (V_m) of P_2O_5 -PbO-BaO glass samples are listed in Table(1) by using equations (1) and (2). Variation of density and molar volume with BaO content is shown in Fig.1. It is observed that the density decreases, and molar volume increases with increasing BaO contents. Although a small kink is observed in both density and molar volume at x=5mol%, some structural change occurs in the glasses under study.

Table 1: Composition, density, and molar volume for P_2O_5 -PbO-BaO glasses

BaO mol %	$\rho(\text{gm/cm}^3)$	$V_m \text{ gm/mol}$
5	1.618	100.58
10	1.518	107.58
15	1.317	124.422
20	1.095	150.15

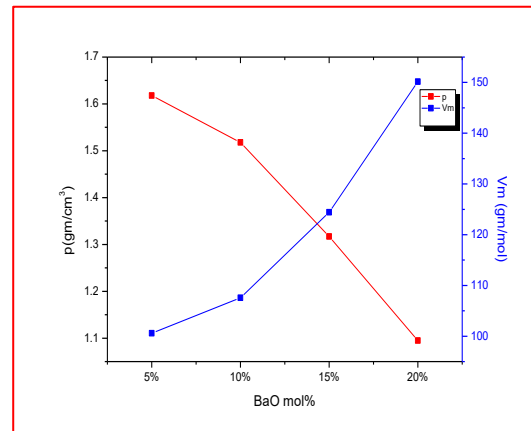


Fig. 1: Relative density and molar volume against BaO content in P_2O_5 -PbO-BaO glasses

Table (2)and Fig. 2. Show the variation of density and molar volume of the P_2O_5 -PbO-MgO glass sample. As shown from the figure, the density increases, and molar volume decreases with increasing MgO contents.

Table 2: Composition, density, and molar volume for P_2O_5 -PbO-MgO glasses

MgO mol %	$\rho(\text{gm/cm}^3)$	$V_m \text{ gm/mol}$
5	1.073	146.41
10	1.0866	139.89
15	1.09	134.78
20	1.108	127.99

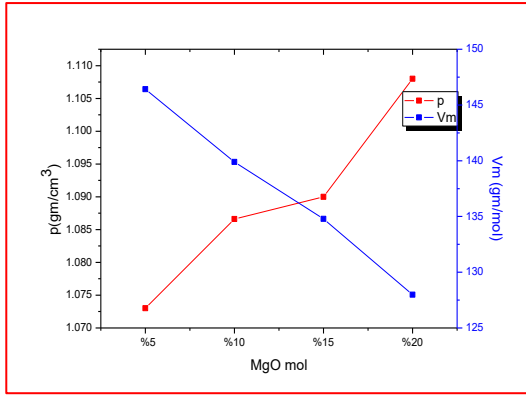


Fig. 2: Relative density and molar volume against MgO content in P₂O₅-PbO-MgO glasses

It is observed from the table (3) that the density of P₂O₅-PbO-CaO glass samples increases from 1.091g/cm³ to 1.13g/cm³ with increasing CaO contents from 5mol% to 20mol% while the molar volume decreases from 144.73 cm³/mole to 128.33 cm³/mole. Figure (3) shows such variation for the P₂O₅-PbO-CaO glass sample.

Table 3: Composition, density, and molar volume for P₂O₅-PbO-CaO glasses

CaO mol %	ρ (gm/cm ³)	V_m gm/mol
5	1.091	144.73
10	1.103	139.26
15	1.12	130.63
20	1.13	128.33

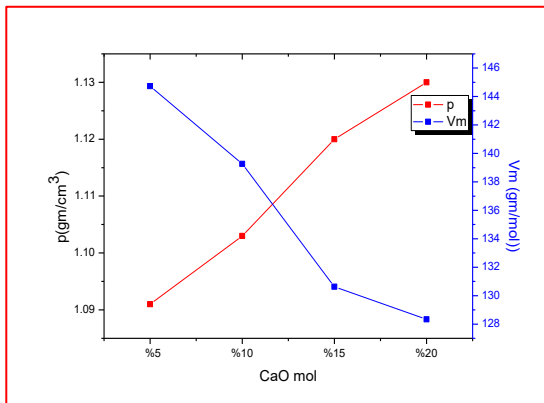


Fig. 3: Relative density and molar volume against CaO content in P₂O₅-PbO-CaO glasses

The observed changes in the structure may be due to the conversion of PO₃ to PO₄ structure units, creating non-bridging oxygens (NBO), which essentially alters the glass structure. The changes in density modified the geometrical construction in the glass network [20].

B. X-Ray Diffraction (XRD)

X-ray diffraction is a quite useful technique because it can detect it readily crystals in a glassy matrix if the crystals are of dimensions greater than typically 100nm[21]. The X-ray diffraction pattern of an amorphous material is distinctly different from that of a crystalline material and consists of a few broad diffuse haloes rather than sharp rings. All glass samples were tested, and the result showed the absence of crystalline characteristics Fig.4 shows typical XRD patterns of simple glass show a broad halo hump 10° to 40°. The presence of broad halo hum at a low angle and the absence of crystalline peak existence indicates that the glass samples are amorphous

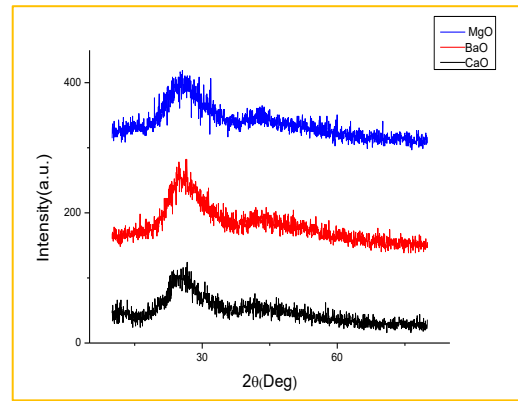


Fig.4: X-ray diffraction patterns of three samples of lead-phosphate glasses

C. Optical Absorption edge Measurements

a) Optical absorption of P₂O₅-PbO-BaO glasses

The optical absorptions spectra of P₂O₅-PbO-BaO glasses in the visible and near-ultraviolet range are shown in Fig.5. The position of the fundamental absorption edge shifts to lower energy with increasing BaO contents.

The absorptions coefficient $\alpha(\omega)$ was determined at different photon energies near the absorptions edge using equation (5). Fig.6 shows a linear dependence of $(\alpha\hbar\omega)^{1/2}$ on photon energy ($\hbar\omega$) for such a glass system in the high photon energy range, and they tend to deviate from linearity at low values of photon energy. The values of the optical energy gap (E_{opt}) are obtained by extrapolating the linear region of the plots to $(\alpha\hbar\omega)^{1/2}=0$ and these values are given in table (4). Fig.7 shows the variation of $\ln\alpha(\omega)$ with photon energy ($\hbar\omega$) for some P₂O₅-PbO-BaO glasses. The values of (E_o) calculated from the slope of the straight lines of these curves are listed in the table (4). For the glass investigated in the present study, the exponential behavior is observed, and the value of (E_o) varies between 0.38eV and 0.59eV depending on BaO contents in the glass composition. This variation is shown in Fig.8. In the present study, the variation of (E_{opt}) with BaO content shown in Fig.9 suggests that the non_bridging oxygen ion content decreases with increasing BaO content shifting the

band edge to lower energies and decreasing the value of (E_{opt}).

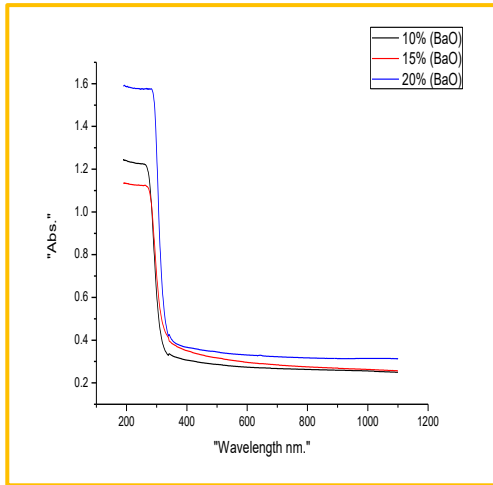


Fig. 5: Optical absorption spectra of P₂O₅-PbO-BaO glasses

Table 4: Optical energy band, Urbach energy, refractive index, and molar refraction for P₂O₅-PbO-BaO

Mol % BaO	E_{opt}	E_o	n	R _m g/mol
10	3.7	0.471	1.9	50.05
15	3.62	0.59	1.92	58.78
20	3.6	0.38	1.925	71.20

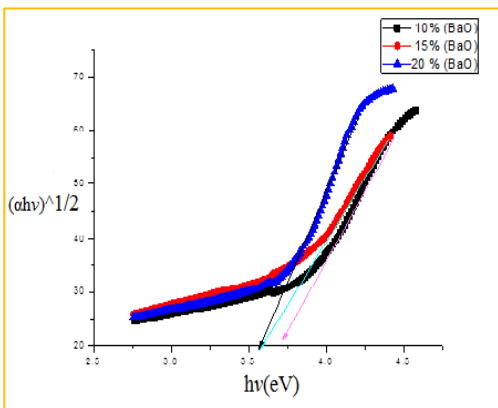


Fig. 6: $(\alpha h\nu)^{1/2}$ is plotted against photon energy for P₂O₅-PbO-BaO glasses

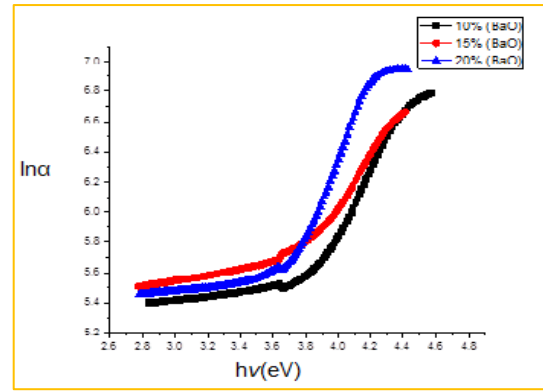


Fig.7: variation of $\ln(\alpha)$ with photon energy for P₂O₅-PbO-BaO glasses

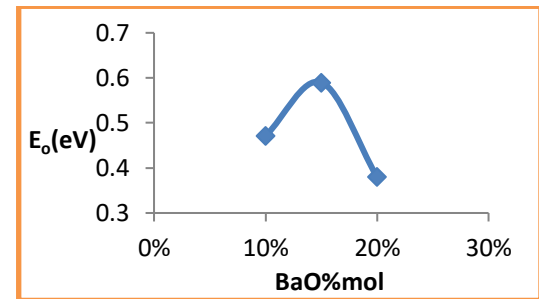


Fig.8: variation of Urbach energy (E_o) with BaO content in P₂O₅-PbO-BaO glasses

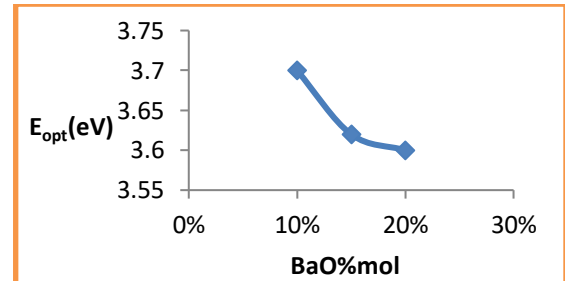


Fig.9: variation of optical band energy (E_{opt}) with BaO content in P₂O₅-PbO-BaO glasses

Refractive index (n) and the molar refraction (R_m) have been determined by using equations (6) and (7), respectively. The values of the refractive index and molar refraction are presented in Table (4). It can be observed that the refractive index and molar refraction are both increasing with increasing BaO content in glass system. Fig. 10 shows such variations.

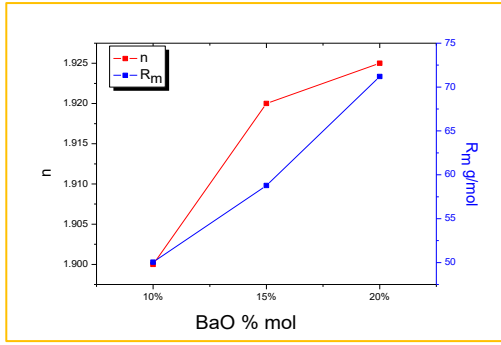


Fig.10: variation of refractive index (n) and molar refraction (R_m) with BaO content in P₂O₅-PbO-BaO glasses

b) Optical absorption of P₂O₅-PbO-MgO glass system
 The optical absorption coefficient measurements, particularly near the fundamental absorption edge, provide a standard method for the investigation of optically induced electronic transitions and provide some ideas about the band structure and energy gap in both crystalline and non-crystalline materials [22].
 The optical absorption measurements were carefully made as a function of photon energy at room temperature. Fig. 11 shows measurements of absorbance against wavelength for a glass of different compositions. Fig. 12 shows the plots of $(\alpha\hbar\omega)^{1/2}$ against the photon energy ($\hbar\omega$) for various compositions of the glasses listed in the table (5).

Table 5: Optical energy band, Urbach energy, refractive index, and molar refraction for

P₂O₅-PbO-MgO

MgO % Mol	E _{opt}	E _o	n	R _m g/mol
5	3.71	0.3	1.9	68.12
10	3.68	0.34	1.91	65.59
15	3.5	0.39	1.94	64.62
20	3.42	0.4	1.95	61.82

The straight lines suggest that the absorption follows the quadratic relation for Davies and Mott's inter band transitions [18]. The optical band gaps were obtained by extrapolating the linear parts of these curves of $(\alpha\hbar\omega)^{1/2}=0$. As shown in Fig.13 and Table (5), there is a systematic decrease in the value of E_{opt} with MgO composition, which suggests that the degree of disorder in these glasses is increased. This supports Mott and Davis [2], which suggests that the extent of the localized states near the mobility edge increases with the increase of disorder in the amorphous structure.

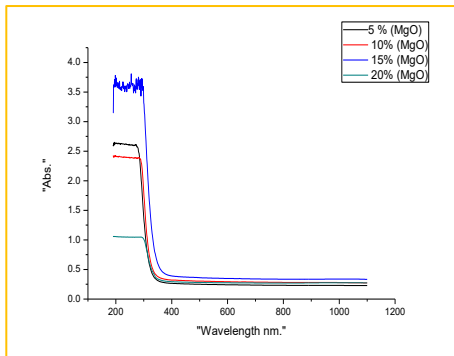


Fig.11: Optical absorption spectra of P₂O₅-PbO-MgO glasses

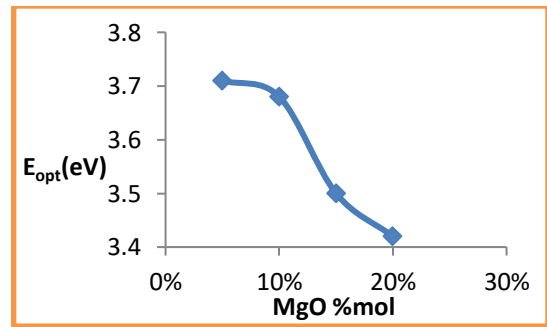


Fig.13: variation of optical band energy (E_{opt}) with MgO content in P₂O₅-PbO-MgO glasses

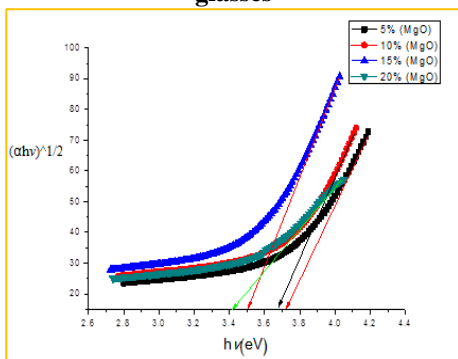


Fig.12: $(\alpha\hbar\omega)^{1/2}$ is plotted against photon energy for P₂O₅-PbO-MgO glasses

In conclusion, as MgO is added to the glasses, deeper band tails are extended in the gap, leading to an increase in the value of (E_o) and a decrease in the matter (E_{opt}). Fig. 14 shows the absorption coefficient as a function of photon energy for different composition of MgO. The values of (E_o), which are determined from Fig.14 by using equation (3), are tabulated in Table (5). Fig.15 shows the increase in the width of the localized states' band tails with increasing MgO content.

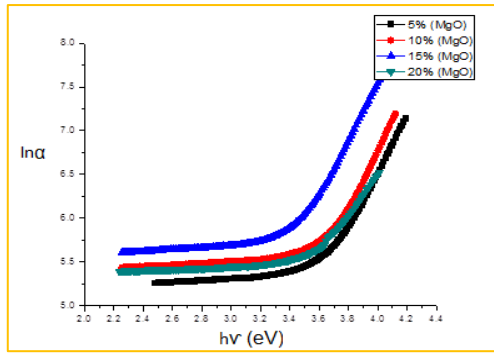


Fig.14: variation of $\ln(\alpha)$ with photon energy for P_2O_5 - PbO - MgO glasses

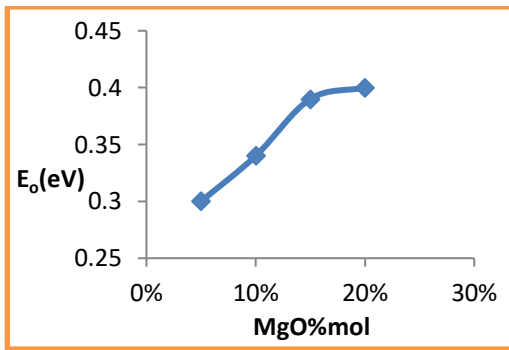


Fig.15: variation of Urbach energy (E_0) with MgO content in P_2O_5 - PbO - MgO

The Refractive index and molar refractivity were calculated and tabulated in Table (5). Fig.16 shows that the refractive index(n) increases, and molar refractivity (R_m) decreases with increasing MgO concentration in the glass network.

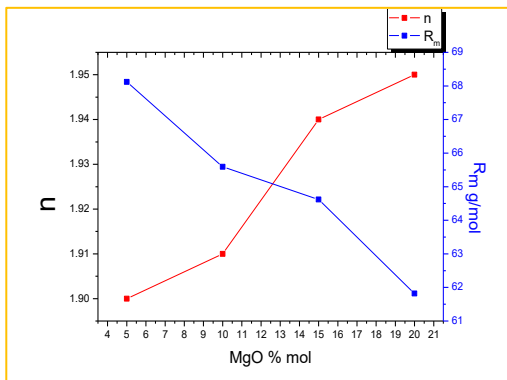


Fig.16: variation of refractive index (n) and molar refraction (R_m) with MgO content in P_2O_5 - PbO - MgO glasses

c) Optical absorption of P_2O_5 - PbO - CaO glass system

Fig.17 shows the typical absorption spectrum of lead-phosphate oxide glasses containing CaO . The absorption coefficient, $\alpha(\omega)$, was determined near the absorption edge at different photon energies for all investigated glass samples. The most satisfactory results were obtained by

plotting the quantity $(\alpha h\nu)^{1/2}$ as a function of photon energy ($h\nu$), as Davis and Mott[18]. Fig. 18 shows the plot of $(\alpha h\nu)^{1/2}$ against $(h\nu)$ for various compositions and the equivalent Urbach plot is presented in Fig. 19 in which absorption coefficients are plotted as a function of photon energy ($h\nu$). From such an exponential edge, the localized states' band tails' width is estimated and listed in the table (6).

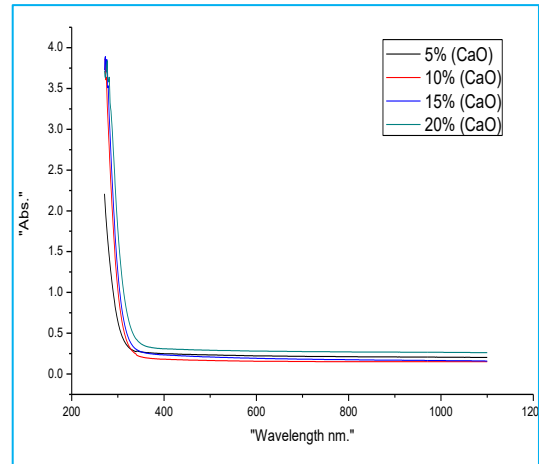


Fig.17: Optical absorption spectra of P_2O_5 - PbO - CaO glasses

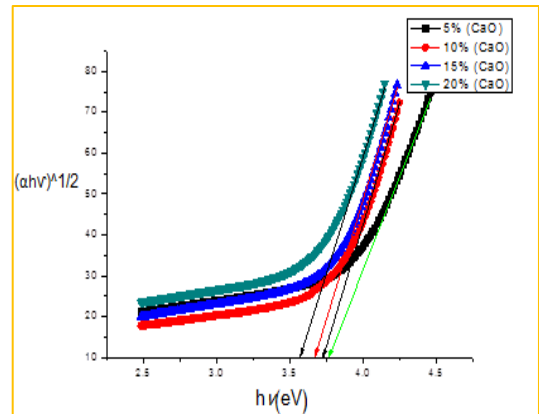


Fig.18: $(\alpha h\nu)^{1/2}$ is plotted against photon energy for P_2O_5 - PbO - CaO glasses

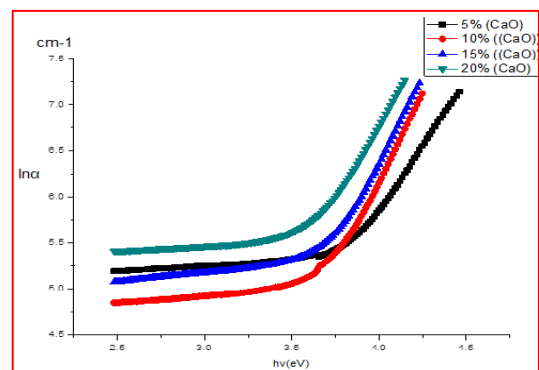


Fig.19: variation of $\ln(\alpha)$ with photon energy for P_2O_5 - PbO - CaO glasses

Table 6: Optical energy band, Urbach energy, refractive index, and molar refraction for

P₂O₅-PbO-CaO

%CaO Mol	eV)(E _{opt}	E _o (eV)	n	R _m g/mol
5	3.76	0.35	1.89	66.81
10	3.73	0.26	1.9	64.79
15	3.68	0.3	1.91	61.25
20	3.59	0.32	1.92	60.63

The values of (E_{opt}) determined from Fig. 18 by extrapolating the linear parts of the curves to $(\alpha\hbar\omega)^{1/2} = 0$ lie within limits between (3.59 to 3.76) eV, and these values may be compared with the values of (E_{opt}), which are different for different compositions. As shown in Fig. 20 and Table (6), there is a systematic decrease in (E_{opt}) values with CaO content in the glass sample. Fig. 21 shows the variation of (E_o) with CaO content.

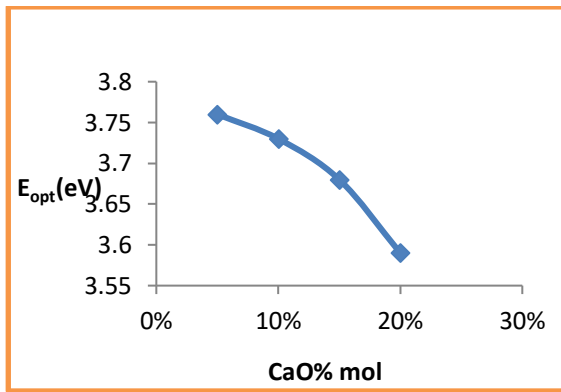


Fig.20: variation of optical band energy (E_{opt}) with CaO content in P₂O₅-PbO-CaO glasses

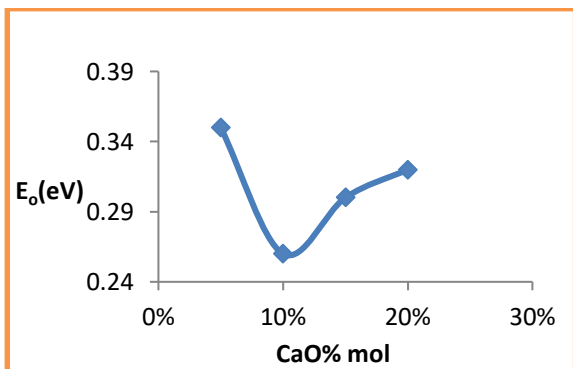


Fig.21: variation of Urbach energy (E_o) with CaO content in P₂O₅-PbO-CaO

The Refractive index (n) depends on the composition of an optical material. Molar refraction (R_m) and refractive index (n) depend on the polarizability of the material. As can be seen from Table (6) and Fig.22 refractive index increases with increasing concentration of CaO in the glass samples,

while the molar refraction decreases with increasing CaO content.

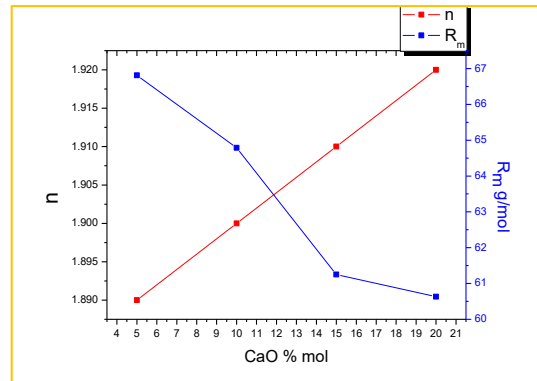


Fig.22: variation of refractive index (n) and molar refraction (R_m) with CaO content in

P₂O₅-PbO-CaO glasses

D. Infrared Spectroscopy

a) Infrared absorption of P₂O₅-PbO-MgO glasses

Infrared Spectra of P₂O₅-PbO-MgO glasses are shown in Fig.23. Table(7) shows the positions of the absorption bands obtained in these glasses. The absorption band at (445-570)cm⁻¹ appears in these glasses and corresponds to the absorption bands at 500cm⁻¹ in crystalline P₂O₅, which is known to be at the fundamental frequency of the (PO₄)⁻³ group [23]. The absorption band at (738-758)cm⁻¹ can be attributed to the (P-O-P) ring frequency, where the absorption band at (1058-1083)cm⁻¹ can be referred to (P-O) stretching frequency. The absorption band at (1259-1280)cm⁻¹ can be assigned to the (P=O) double bond's stretching vibration. The band position at (1640-1666)cm⁻¹ in all glass samples is due to KBr powder's moisture. The identification came from an infrared test carried out on KBr powder, which showed the same absorption band positions. The absorption band at (889-895)cm⁻¹ is due to the Pb-O bond. The absorption band at (3437-3452)cm⁻¹ was observed for these glasses. This was believed to be caused by a small amount of water in the glass.

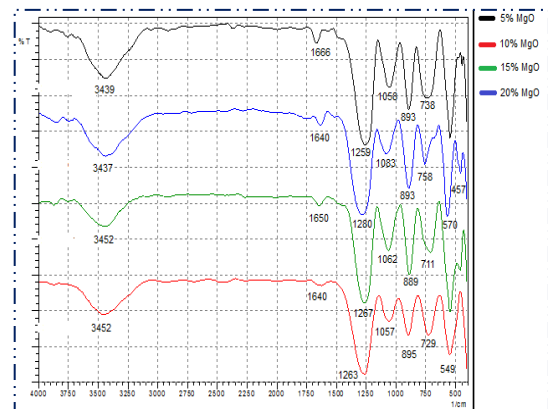


Fig.23: Infrared absorption spectra in P₂O₅-PbO-MgO glass

Table 7: Band positions in P₂O₅-PbO-MgO glasses

MgO%mol content	Band position (cm ⁻¹)							
	400	500	750	900	1000	1250	1600	3500
5	445	545	738	893	1058	1259	1666	3439
10		549	729	895	1057	1263	1640	3452
15	461	547	711	889	1062	1267	1650	3452
20	457	570	758	893	1083	1280	1640	3437

b) Infrared absorption of P₂O₅-PbO-BaO glasses

Spectra were obtained on glass with BaO concentrations varying from (5 to 20 mol%) with negligible shifts in band positions. The IR spectra of the P₂O₅-PbO-BaO glasses are shown in Fig. 24. Table (8) shows the position band of these glasses. It has been shown that most of the absorption bands in the glasses are the same as for P₂O₅. The absorption band at (424-563)cm⁻¹, which appears in such glasses corresponding to the fundamental frequency of the (PO₄)⁻³ for crystalline P₂O₅ [23]. The absorption bands at (702-777)cm⁻¹, (1015-1072)cm⁻¹, and (1265-1274)cm⁻¹ could be due to the P-OP ring frequency, P-O stretching frequency, and the stretching vibration of the P=O double bond. The absorption band at (896-902)cm⁻¹ is due to the Pb-O bond. An absorption band at (1520-1651)cm⁻¹ is due to KBr powder [24]. The absorption band at (3416-3489)cm⁻¹ was observed, and this is believed to be due to the small amount of water trapped in the glass.

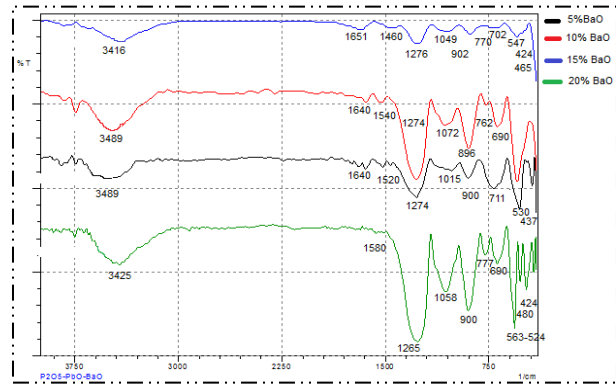


Fig24 : Infrared absorption spectra in P₂O₅-PbO-BaO glasses

Table 8: Band positions in P₂O₅-PbO-BaO glasses

BaO%mol content	Band position (cm ⁻¹)										
	400	450	500	600	750	900	1000	1250	1500	1600	3500
5	437		530	711		900	1015	1274	1520	1640	3489
10			545	690	762	896	1072	1274	1540	1640	3441
15	424	465	547	702	770	902	1049	1267	1460	1651	3416
20	424	480	524 563	690	777	900	1058	1265	1580		3425

c) Infrared absorption of P₂O₅-PbO-CaO glasses

The infrared absorption spectra of four samples were obtained at room temperature in the wavenumber range (4000_400)cm⁻¹. The infrared spectra of the glasses are shown in Fig.25. Table (9) shows the positions of the absorption bands obtained in these glasses. The band position (434_570)cm⁻¹ is due to (PO₄)⁻³ group [23]. The absorption band at (769_704)cm⁻¹ is due to the P-O-P ring frequency. The absorption band at (1051_1057)cm⁻¹ can be attributed to

P-O stretching frequency, where the absorption band at (1261_1267)cm⁻¹ is due to the P=O double bond. The absorption band, which appears at (900_916)cm⁻¹ is due to the Pb-O bond. An absorption band at (1524_1535)cm⁻¹ is due to KBr powder's moisture as assigned before [24]. Finally, the absorption band at (3427_3435)cm⁻¹ was believed to be caused by a small amount of water in the glass.

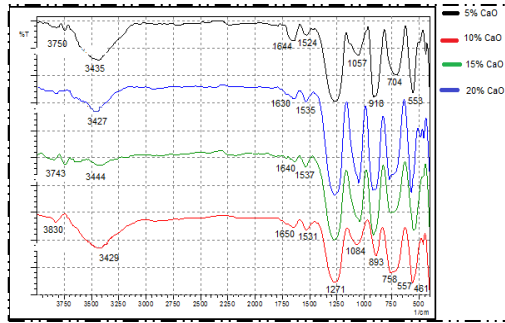


Fig.25: Infrared absorption spectra in P₂O₅-PbO-CaO glasses

Table 9: Band positions in P₂O₅-PbO-CaO glasses

CaO%mol content	Band position (cm ⁻¹)									
	400	500	750	900	1000	1250	1500	1600	3500	3750
5	434	553	704	918	1057	1271	5241	1644	3435	3750
10	461	557	758	893	1084	1271	1531	1650	3429	3830
15	459	547	750	916	1043	1273	1537	1640	3444	3743
20	453	570	769	900	1051	1267	1535	1630	3427	

The density measurements of P₂O₅-PbO-BaO glasses decreases from 1.618 g/cm³ to 1.095 g/cm³ while the molar volume increases from 100.58 g/mol to 150.15 g/mol with an increment of BaO content. The decrease in density may be attributed to the lower molecular mass of BaO compared to the larger molecular mass of P₂O₅. Besides that, another reason is the creation of non-bridging oxygen, which essentially alters the glass structure. The density of P₂O₅-PbO-CaO and P₂O₅-PbO-MgO glasses increases with the increase of CaO and MgO contents. As expected, CaO and MgO's addition to the phosphate network causes some type of structural rearrangement of the atoms. There is a possibility of altering the geometrical configuration upon the substitution of CaO and MgO into the glassy phosphate network.

The decreases in the molar volume in such glasses are due to the decrease in the bond length or inter-atomic spacing between the atoms, which may be attributed to the increase in the bonds' stretching force inside the glass network.

The increase in the refractive index with an increase of BaO, MgO, and CaO contents related to the decrease in the energy band gap and relates to the glass's compactness. Furthermore, an increase in the refractive index also due to alteration in the glass network. Incorporation of BaO, MgO, and CaO contents modified phosphate and oxygen structure, which alter the glass network by introducing more formation of non-bridging oxygen at the expense of bridging oxygen.

The variations of (E_{opt}) with BaO, MgO, and CaO contents show that the indirect bandgap values decrease with increasing MgO, BaO, and CaO contents in the glass network. Those results suggest that the glass matrix's

covalent nature decreases with increased MgO, BaO, and CaO contents.

As shown from tables (4,5,6), the values of (E_{opt}) decrease with BaO, MgO, and CaO contents. Such variations can be explained by suggesting that the non-bridging oxygen ion content increases with an increase of MgO, CaO, and BaO contents shifting the band edge to higher energies and leading to a decrease in the values of (E_{opt}).

As can be seen from the infrared absorption spectra of lead-phosphate glasses, these spectra are similar to the infrared absorption spectrum of crystalline P₂O₅, which suggests that the phosphate tetrahedral are dominating the structure of these glasses.

Most of the absorption bands seen in the present study are in close agreement with many researchers [24_28].

IR spectra of all the samples showed large water peaks. This moisture effect could disrupt the whole spectrum and add general noise. It would be useful to remove these peaks to improve the results obtained from IR spectra. One way of removing the water is by heating the sample for about 2hours before the IR measurements.

References

[1] Hassan, M.A., Khleif, W.I, Hogarth, C.A., J.Mat.Sci, 24, 1607-1611(1989).
 [2] Mott, N.F. and Davis, E.A., "Electronic Processes in Non-crystalline Materials." (Oxford Univ. Press)2nd.(1979)
 [3] Freibebe, E.J, Griscom, D.L., Treatise on Materials science and Technology, Academic Press, New York, (1979).

- [4] Shelby, J.E., Rare Elements in Glasses, Switzerland: Trans Tech Publications, (1994).
- [5] Rami Reddy, M., Ravi Kumar, V., Veeraiah, N., Appa Rao, B., Indian J. Pure Appl. Phys., 33, 48, (1995).
- [6] Saeed, A., Elbashar, Y.H., Elshazly, R.M., Opt. Quantum Electron, 48.1(2016).
- [7] Elbashar, Y.H., Saeed, A., Res. J. Pharm. Bio, Chem. Sci 6, 1830-1837(2015).
- [8] Saeed, A., Elbashar, Y.H., Elkameesy, S.U., Res.j.Pharm., Bio. Chem.Sci., 6, 1830-1837 (2015).
- [9] Ravicumar, R.V., Chandrasekhar, A.V., Journal of Alloys and Compounds, 364, 176-179 (2004).
- [10] Brow, R.K., Tallant, D.R., J. Non-Cryst. Solids, 222, 396-406 (1997).
- [11] Ray, N.H., Lewis, C.J., Lay cock, JN, and Robinson, W.D., Glass Technology, 14, 50-59 (1973).
- [12] Sultan, M.A., Elwhab, O.M., Appl. Phys. A. 123, 1-12 (2017).
- [13] Upender, G., Ramesh, S., Prasad, M., Sathe, V.G., and Mouli, V.C., J.Alloys compd. 504, 468-474 (2010).
- [14] S.L.Meena, "Spectral and Thermal Properties of Ho³⁺ Doped Aluminum- Barium- Calcium-Magnesium Fluoride Glasses" SSRG International Journal of Applied Physics 7.1 (2020): 14-20.
- [15] Yaacob, S.N.S., Sahar, M.R., Sazali, E, S, and Sulhadi, S., Solid-state phenomena, 290, 35-40 (2019).
- [16] Urbach, F., *Physi. Rev.*, 92(5), 1324. (, 1953).
- [17] Hassan, M.A., Hogarth, C.A., J.Mat. Sci., 23, 2500-2504 (1988).
- [18] Davis, E. A., & Mott, N.F., *Phil. Mag.*, 22, 903 (1970).
- [19] Eraiah, B., *Bull. Mat. Sci.*, 29, 375-378. (, 2006).
- [20] Satyanarayana, T., Nagarjuna, G., Ravikiran, K., Solid-state phenom., 207, 55-67 (2014).
- [21] Anderson, G.W., Luhrs, W.D., *J.Appl. Phys.*, 39, 1634 (1968).
- [22] Hassan, M.A., Khan, M.N., Hogarth, C.A., *Phys. Stat. sol.*, 105,609, (1988).
- [23] Richard, A. Nyquist, and Ronaldo. Kagel, "*Infrared spectra of inorganic compounds*" (New York & London), (1971).
- [24] Dogra, Mridula, et al., *European Journal of Glass Science and Technology Part B*, 59, 293-300 (2018).
- [25] Doweidar, H., et al., *Vibrational spectroscopy*, 37, 91-96 (2005).
- [26] Dayanand, C. et al., *J.Mat. Sci.*, 31, 1945-1967 (1996).
- [27] Kumar, Valluri Ravi, G. Giridhar, & Veeraiah, N. *Luminescence*, 32, 71-77 (2017).
- [28] Shereen, A., Hassan, M.A., Kirkuk Univ., *J. Sci. Stud.*, 11, 100-114 (2016).
- [29] El-mallawany, R., *J.Appl. Phys.*, 72, 1774, (1992).